OFFICE OF NAVAL RESEARCH

Grant N00014-89-J-1261

R&T Code 4131038

ONR Technical Report ONR Technical Report #32

Surface Structural Studies of Methane Sulfonic Acid at Air/Aqueous Solution Interfaces using Vibrational Sum Frequency Spectroscopy

by

H.C. Allen, E.A. Raymond, and G.L. Richmond

Journal of Physical Chemistry, submitted

Department of Chemistry
1253 University of Oregon
Eugene, OR 97403

July 2000

REPORT DOCUMENTATION PAGE

Form Approved
OMB No. 0704-0188

1. AGENCY USE ONLY (Leave Blank)	2. REPORT DATE	3. REPORT TYPE AND DATES COVERED
	10 July 2000	Technical 6/1/99-5/31/00

4. TITLE AND SUBTITLE
Surface Structural Studies of Methane Sulfonic Acid at Air/Aqueous Solution Interfaces using Vibrational Sum Frequency Spectroscopy

5. FUNDING NUMBERS
N00014-89-J-1261

6. AUTHOR(S)
H.C. Allen, E.A. Raymond, and G.L. Richmond

7. PERFORMING ORGANIZATION NAME(S) AND ADDRESS(ES)
Dept. of Chemistry
University of Oregon
Eugene, OR 97403

8. PERFORMING ORGANIZATION REPORT NUMBER
ONR Technical Report #32

9. SPONSORING/MONITORING AGENCY NAME(S) AND ADDRESS(ES)
Dr. Peter Schmidt
Office of Naval Research Physical Science and Technology, ONR 331
800 North Quincy Street
Arlington, VA 22217-5000

10. SPONSORING/MONITORING AGENCY

11. SUPPLEMENTARY NOTES
Journal of Physical Chemistry, submitted

12A. DISTRIBUTION / AVAILABILITY STATEMENT
Approved for public release: distribution unlimited

12B. DISTRIBUTION CODE

13. ABSTRACT (Maximum 200 words)
Please see attached abstract

14. SUBJECT TERMS
Vibrational Sum Frequency Spectroscopy, characterization of air/aqueous interfaces

15. NUMBER OF PAGES
26

16. PRICE CODE

17. SECURITY CLASSIFICATION OF REPORT	18. SECURITY CLASSIFICATION OF THIS PAGE	19. SECURITY CLASSIFICATION OF ABSTRACT	20. LIMITATION OF ABSTRACT
Unclassified	Unclassified	Unclassified	

Surface Structural Studies of Methane Sulfonic Acid at Air /Aqueous Solution Interfaces using Vibrational Sum Frequency Spectroscopy

Allen, H.C.[†], Raymond, E.A., Richmond, G.L.*

Department of Chemistry, University of Oregon, Eugene, OR 97403

* To whom correspondence should be addressed
[†] Postdoctoral fellow for the NOAA Postdoctoral Program in Climate and Global Change
Current address: Department of Chemistry, The Ohio State University, 100 W. 18th Ave., Columbus, OH 43210

Abstract

Atmospheric gas phase species such as methane sulfonic acid (MSA) are adsorbed and accommodated into atmospheric aqueous-phase aerosols and in some cases MSA is thought to be produced via aerosol surface chemistry. The studies described herein probe the surface molecular structure of MSA at aqueous solution surfaces using surface vibrational sum frequency spectroscopy (VSFS). In the studies presented here, it is shown that MSA partitions at the surface and that the surface MSA has a preferred surface orientation in which the MSA methyl group points away from the liquid surface. The surrounding surface water structure is significantly affected by the adsorption of MSA. Small amounts of MSA at the surface of water enhances the intermolecular hydrogen bonding between interfacial water molecules. Additional VSF studies show that MSA is effectively displaced by sulfuric acid at an aqueous surface. The structural details presented here may have implications for understanding atmospheric aerosol growth properties.

Introduction

Adsorption and molecular structure of methane sulfonic acid, MSA (CH_3SO_3H), at an aqueous solution surface are important to study because of the role MSA plays in tropospheric aerosol (liquid and solid particle) chemistry. In addition, studies elucidating MSA surface structure have particular relevance to the understanding of past and future global climate change. Ice core measurements of MSA and non sea-salt sulfate (NSS) concentrations, and MSA : NSS ratios have been used by glaciologists to help understand historical climate trends. An inverse relationship between glacially deposited MSA (originating from the atmosphere) and planetary temperatures has been shown to exist.[1]

In addition to resolving past long-term climate trends, understanding the causal relationships that shape current climate trends are important to the understanding of global climate change. Tropospheric aerosols have been recognized to alter climate by changing the albedo of the atmosphere.[2-4] Tropospheric aerosols are formed by aerosol nucleation, growth and chemical processes in which MSA and NSS are important factors. Therefore, understanding heterogeneous chemical processes is necessary to the understanding of climate change.[5]

In this paper, we present studies of the adsorption and molecular structure of MSA at aqueous solution surfaces. The structure of surface MSA and how that structure changes as a function of concentration in binary aqueous and ternary sulfuric acid aqueous solutions are explored. In addition, measurements examining how the surface water structure changes upon addition of MSA and MSA/sulfuric acid have been made. We find that the hydrogen bonding and free OH modes of surface water are both affected by the presence of surface MSA. The average orientation of surface MSA has also been measured to help understand the factors that influence the resulting surface water structure.

Surface vibrational sum frequency spectroscopy (VSFS) is the primary technique employed in these studies. The surface specificity of this second order nonlinear optical method allows the vibrational spectrum of methane sulfonic acid adsorbed on a water surface to be obtained. This surface sensitivity arises from the noncentrosymmetric nature of the interface that gives rise to a second order nonlinear response, i.e. sum frequency, difference frequency, and second harmonic generation. Recent advances in instrumentation used for VSFS measurements, in particular the use of psec and fsec[6] pulsewidths, have resulted in higher nonlinear efficiencies that lessen the risk of surface damage.[7] By increasing the nonlinear efficiencies, small surface coverage and weak vibrational modes that were below VSFS detection limits for a gas/liquid interface are now more easily observed. In our laboratory these advances and improvements in detection have opened new opportunities for studying atmospheric processes. Our improved spectral resolution, methods for spectral analysis that include the phase of the

VSFS response, and increased sensitivity to submonolayer coverages of atmospherically relevant molecules have made the studies reported herein possible.

Experimental Section

The laser system used in these studies has been previously described.[8,9] A summary of the experimental set-up and recent modifications of this system are detailed below. The production of the 800 nm beam (kHz repetition rate, 2 ps, 1.6 W) begins with a Ti:Sapphire (Coherent Mira) passively mode-locked laser pumped with 5.5 Watts of a 532 nm laser beam from a Coherent Verdi laser. The Mira produces an ~135 fs, 800 nm seed, which is stretched in time to ~ 100 ps and amplified with a Quantronix regenerative amplifier and a double pass Ti:sapphire amplifier, then compressed to 2 ps. The amplifiers are pumped with a total of 12 Watts of a 527 nm kHz YLF laser. The resulting amplified 800 nm laser beam is split by a 75/25 beam splitter. Approximately 25 % of the 800 nm light is used as one of two beams incident at the surface. The infrared pulses are temporally and spatially overlapped with the 800 nm pulses at the sample surface.

The infrared (2700 – 3850 cm^{-1}) is produced from 75 % of the 1.6 Watt 800 nm beam via a home-built optical parametric amplifier (OPA) system. The OPA consists of 2 angle tuned KTP (potassium titanyl phosphate) crystals. Recent changes to this system from previous work[8,9] include the incorporation of a 2 cm length $MgO:LiNbO_3$ crystal that is used as the optical parametric generator (OPG) from which the resultant 1 – 1.2 micron wavelengths are used to seed the first KTP crystal. We employ a grating for the selection of the seed wavelength. The infrared is generated by seeding the first KTP crystal and then amplifying through the second KTP crystal. Each KTP crystal is pumped with ~0.450 mJ of the 800 nm beam. The resultant infrared frequencies are scanned as a function of time. The 800 nm beam, focused approximately 1 cm before the interface (~0.5 mm spot size at the interface), and the infrared beam, focused to ~0.3 mm at the interface, are temporally and spatially overlapped at the solution surface. The 800 nm and infrared beams are incident at ~56 degrees and 67 degrees from the surface normal, respectively. The reflected sum of the two incident frequencies (at ~ 630 nm) is detected

with a cooled CCD camera (Princeton Instruments) after spatial filtering and use of polarization and wavelength selection optics. Spectra are normalized by dividing the SF intensity by the infrared power, which takes into account the changes in infrared intensity as a function of wavelength. In all regions of the spectrum, calibration of the monochromator with different order HeNe lines preceded the calibration of the spectrum by the monochromator.

The intensity of the SF is proportional to the square of the orientationally-averaged molecular number density in the interfacial region. Resonant SF intensity is generated at an interface when the infrared frequency is resonant with a Raman and infrared-active vibrational mode of molecules in the interfacial region. Since VSF is a coherent process, the SF response from vibrational modes of nearby frequencies can constructively, and in some cases, destructively interfere with one another. Spectra presented here were obtained using the SSP and SPS polarization combinations (e.g. SSP - S polarized SF, S polarized 800 nm beam, and P polarized infrared beam). The SSP polarization combination provides data on surface IR-active vibrational modes that have components of their transition moments parallel to the surface normal and the isotropic Raman response from the interface. The SPS polarization combination provides data on surface IR-active modes with transition moment components parallel to the surface plane and the anisotropic Raman response.

Presented spectra were taken at room temperature (~ 293 K). Surface exposure to atmospheric gases and contaminants are an issue when samples are exposed to the outside environment for any period of time. Therefore, a fresh sample is examined for each VSF spectrum taken.

Water used in the experiments is Aldrich HPLC grade. ACS + grade methane sulfonic acid, 99 %, and sulfuric acid, 96+ % solutions were obtained from Aldrich. Surface tension was measured using the Wilhelmy plate method and has been described previously.[10]

Results and Discussion

The results and discussion section are organized in the following manner. Surface tension data of MSA in purely aqueous solutions is discussed in section I to determine surface MSA concentration for various bulk MSA concentrations. Section II describes the VSF spectrum of neat water prior to addition of MSA. This is followed by the VSF results of these surfaces at different MSA/water mixtures (section III). In section IV, VSF spectra of concentrated sulfuric acid, binary, and ternary solutions are compared. This includes SSP VSF spectra of MSA / water solutions, and MSA / sulfuric acid (SA) / water solutions which are discussed in terms of surface displacement and preferential surface species.

I. Surface tension measurements of MSA aqueous solutions

To understand the surface adsorption properties of aqueous MSA solutions, the surface tension of MSA was studied as a function of MSA concentration in water. In Figures 1a and 1b, measured surface tension (0 to 1.0 mf MSA) and calculated number densities are plotted versus mole fraction of MSA in water. The 2-dimensional bulk density is calculated from the density of MSA ($\rho^{2/3}$) in order to compare it with the MSA surface excess, which is also in units of molecules/m^2. The surface excess of MSA is the calculated number of molecules in excess compared to the bulk density. The MSA surface number density is the bulk density added to the surface excess.[10] We have used mole fraction values for surface excess data due to the lack of published activity data for MSA. Figure 1a shows that the surface tension decreases with increased amounts of bulk MSA concentration. The surface tension does not change significantly beyond 0.3 mf MSA. Figure 1b displays MSA bulk number densities and MSA surface excess and the MSA surface number densities in the low concentration regime. These values were determined using the surface tension data of Figure 1a and the Gibbs equation. A linear increase is observed for the bulk number density as a function of MSA mole fraction. In contrast, the surface excess and the surface number density are observed to increase steeply at the low concentrations with a slower increase observed at higher concentrations.

The results of Figure 1b indicate a strong partitioning of MSA at the surface. MSA surface number densities are 7.7 and 7.9 times higher than their corresponding bulk densities at 0.02 and 0.03 mf MSA, respectively. At 0.02 mf MSA and at 0.03 mf MSA the effective surface-concentration is 0.15 mf_e MSA and 0.24 mf_e MSA, respectively. In a bulk 0.03 mf MSA solution this translates into 24 MSA to 75 water molecules at the surface (surface ratio of ~ 1 : 3) whereas in the bulk there are 3 MSA molecules for every 97 water molecules (bulk ratio of 1 : 32). At bulk concentrations of 0.1 mf MSA (bulk ratio of 1 : 9) the magnitude of the difference between bulk and surface concentrations begins to decrease. At this concentration the surface number density is only 5 times higher, giving a surface mf_e of 0.5 (surface ratio of 1 : 1). The MSA surface population exceeds the surface water population for bulk concentrations greater than 0.10 mf MSA. The surface number density (number of molecules per unit surface area) of highly soluble molecules is proportional to the bulk density of its solution with some dependence on relative surface tensions,[11] but as shown in Figure 1b, the MSA surface and 2-dimensional bulk density are not the same.

Generally, adsorbed organic solutes are known to decrease the surface tension of water. Although highly soluble organic solutes can moderate this effect, these molecules can still partition effectively to the surface of an aqueous solution. Previous surface tension studies of dimethyl sulfoxide (DMSO) show significant surface paritioning of DMSO from aqueous solutions.[10] This was attributed largely to the nonpolar methyl groups that prefer the surface region over the highly polar aqueous phase.[11] Methyl (and methylene) groups do not induce strong hydrogen bonding, therefore, it is more thermodynamically favorable for a molecule at an air/aqueous interface to have its hydrophobic moiety protruding into the air phase of the interfacial region, while the hydrophilic group (e.g. SO_3H group of MSA) is solvated by the H_2O. We conclude that this gives rise to the surface partitioning characteristics that have been observed here for MSA.

II. VSF of the vapor/water interface

To understand how the adsorption of MSA alters the hydrogen bonding of water at the air/ water interface, it is first necessary to examine the VSF spectrum of water at a neat air/water interface. Although the VSF spectrum of the air/water interface has been measured in previous studies, [12-22] new insights are provided in these studies that justify acknowledgement. Furthermore, given that several groups have now published VSF spectra for the air/water interface that have significant differences, a comparative analysis of these differing results is warranted and presented here. Figure 2 shows the VSF spectrum of surface water taken from HPLC-grade water (pH = 6.5) using SSP polarization. The spectral assignments for liquid water are somewhat controversial due to the broadness of the peaks and the continuum of states in the bulk liquid. Thus, we assign our intensity regions for the VSF surface spectrum with some caution in that we utilize IR and Raman assignments taken from bulk water measurement. The surface water spectrum has the general shape of an isotropic Raman bulk water spectrum, yet there are important differences. Consistent with Raman and infrared pH data and cluster studies, the VSF intensity in the 2900 cm^{-1} ($\pm$ 150 cm^{-1}) broad region is attributed to two different phenomena, either assignment to cationic and anionic water species, i.e. H_3O^+, $H_5O_2^+$, or $H_3O_2^-$.[23,24] or to various cluster distribution effects.[25] It is likely that both of these phenomena are contributing to the SF intensity since ionic species tend to partition to an aqueous surface, and clustering of surface water species is probable. The broad band from approximately 3000 to 3600 cm^{-1} is assigned to the broad distribution of OH hydrogen bonding stretching modes in which the oxygen is tetrahedrally coordinated.[26-31] The energy region from ~3000 - 3250 cm^{-1} is attributed to strong intermolecular in-phase hydrogen bonds of water molecules which give rise to a highly correlated hydrogen bonding network. This region is dominated by a continuum of OH symmetric stretches, ν_1. The higher energy broad band region (~3250 - 3500 cm^{-1}) is assigned to more weakly correlated hydrogen bonding stretching modes of molecular water that encompass both ν_1 (OH symmetric stretch) and to a lesser extent, ν_3 (OH asymmetric stretch) vibrational modes. We observe a slight decrease in VSF intensity centered at ~3250 cm^{-1} which could be attributed to a Fermi resonance of the ν_1 OH stretching modes

with the overtone OH bending modes, $2\nu_2$,[31] or to the isosbestic point postulated to exist for bulk water.[32,27,33] The distinct peak at 3702 cm^{-1} is assigned to the dangling OH bond with the oxygen hydrogen-bonded to 3 and 2 subsurface-coordinated molecules, $OH_{(da)}$.[34,28] The terminal hydrogen of the dangling $OH_{(da)}$ bonds are not involved in hydrogen bonding to other condensed phase molecules and has also been referred to as the free OH.[15] The shoulder at ~3760 cm^{-1} is assigned to the asymmetric stretch (AS) of the interfacial vapor state water species. The detection of the vapor state species has been discussed in a previous paper.[12]

Differences, and in some cases, similarities in relative intensities of modes are observed from the surface-water spectrum in Figure 2 compared to Raman and infrared studies of bulk water. The dominant difference relative to bulk studies is the significant SF intensity in the 2900 cm^{-1} region of the VSF spectrum. The VSF intensity in the 2900 cm^{-1} region is more intense relative to both the infrared and the Raman (isotropic) intensity previously observed in the 2900 cm^{-1} for neat bulk water.[31,23] Recall that the SSP VSF intensity is a function of both the isotropic Raman polarizability and the infrared transition moment and that the SF process is coherent which can alter the shape of the resultant spectrum.[35,36] Taking the coherent nature of SF into account by allowing for interference effects, we still observe a distinct difference in the VSF spectrum of surface water compared to the Raman and infrared spectra of bulk water. There are two possible explanations for this, either highly cooperative water cluster distributions[25] or surface water species with ionic character,[23,24] as mentioned above.

In addition to comparison of surface spectra with bulk Raman and infrared spectra, it is important to compare our VSF spectra with the surface water VSF spectra obtained in other studies. There have been several SSP (out-of-plane) VSF spectra from air/water interfaces published.[13-22] Although these published VSF spectra have general similarities, there are some notable differences, as might be expected from the different laser systems used and the difficulty in acquiring the VSFS data. In the region from 2900 to 3600 cm^{-1}, our VSF spectrum of surface-water is similar to VSF surface-water spectra

published by Shen and coworkers,[13-15] which also shows intensity in the ionic/cluster water species region (~2900 cm^{-1}), the inflection region near 3250 cm^{-1}, and a relatively large intensity contribution in the 3190 cm^{-1} region. Although the shape is generally similar, we observe a sharper peak intensity at 3190 cm^{-1}. Shultz and coworkers using a nanosecond laser system observe this peak at 3150 cm^{-1}.[16-19] The intensity drop at 3600 cm^{-1} observed here is consistent with the work of Shen and coworkers.[13-15] The SF intensity drop to nearly zero observed at 3220 cm^{-1} by Shultz and coworkers[16-19] is not observed in either our work or the studies by Shen and coworkers,[13-15] nor is the weakness of the intensity at 3550 cm^{-1}. One possible explanation for the differences between the air/water spectra of Shultz and the other studies is that the former uses a nanosecond laser system instead of the picosecond lasers of this group and Shen.

There are also similarities and differences of the VSF spectra in the free OH region (~3700 cm^{-1}) from different groups. In the $OH_{(da)}$ (free OH) bond region, we observe this peak at 3702 cm^{-1} ($\pm$ 6 cm^{-1}). The infrared frequency was carefully calibrated for this spectral assignment with the details given in the Experimental section. This free OH assignment is in reasonable agreement with Buch and Devlin[34,28] in which the $OH_{(da)}$ mode is observed at 3696 cm^{-1} and 3720 cm-1 for 3- and 2-coordinate surface water molecules for amorphous ice surfaces. The literature is somewhat scattered for the free OH assignment from VSF spectra, in which assignments range from 3670 to 3710 cm^{-1},[13-22] yet all results agree reasonably within this range. VSFS intensities differ for the free OH region depending on the laser system utilized and differences are easily explained by laser pulse temporal dephasing. For our 2 ps laser system in the 3700 cm^{-1} (~2.7 microns) region the pulse undergoes free induction decay as a result of interaction with water vapor in the atmosphere (discussed in Gragson et al.[8] and Crowell et al.[37]), which redistributes a portion of the energy into surrounding frequencies and dephases the temporal coherence of the beam in this wavelength region. Because of our 17 cm^{-1} bandwidth (FWHM) an average power is observed, thereby masking the full effect of the intensity absorption and redistribution. This redistribution of energy results in a smaller than expected peak intensity for the 3700 cm^{-1} vibrational resonance in our VSF spectra,

which cannot be accounted for by simply normalizing to the infrared intensity. Consequently, the smaller absolute height of the 3700 cm^{-1} peak is an artifact of the laser and OPA system. From a longer 20 ps pulse, this effect is lessened and with the use of a nanosecond laser, the effects of free induction decay should not be an issue. Additional similarities in this higher energy region include the VSFS detection of the water vapor AS at ~ 3760 cm^{-1} in the work of Allen et al.[12], Du et al.[15], and Shultz and coworkers,[16-22] although not previously recognized as such.[12] It should be noted that the free induction decay discussed above does not affect the frequency measurement for the free OH nor the AS mode of the water vapor.

III. VSF spectra of MSA solutions

Figure 3a is the VSF spectrum of surface MSA for a 99+% MSA liquid. The data was taken with SSP polarizations. The peak at 2947 cm^{-1} (± 6 cm^{-1}) is assigned to the methyl symmetric stretch (CH_3-SS). The SF response from the methyl asymmetric stretch (CH_3-AS) is present but is less obvious. Fits to the data shown in Figure 3b place the AS mode at 3032 cm^{-1}, which is close to that obtained for bulk MSA as measured by Raman and IR (3032 cm^{-1} and 3036 cm^{-1}, respectively).[38] The VSF response from the CH_3-AS and to a lesser extent the broad underlying bands, destructively interfere with the SF response from the CH_3-SS, resulting in an observed decrease in the SF intensity in the 2950 – 3025 cm^{-1} region. By mathematically transforming the hyperpolarizability elements of the SS and the AS of the methyl group of MSA from molecular coordinates to the laboratory coordinate system via Euler angle rotations, it has been shown previously that the SF response from the SS and the AS of CH modes from methyl groups of C_{3v} symmetry are of opposite phase.[36,39,40] That is what is observed here. This interference effect coupled with the 85 cm^{-1} peak to peak separation of modes results in the square-shaped intensity drop that is observed in the VSF spectra of MSA solutions shown in Figures 3 - 5. The shape of the distortion is dependent on the frequency separation of the modes, i.e. smaller frequency separations result in observed sharper dips rather than square intensity drops. The CH_3-AS is small as shown in Figure 3b, but has a

profound impact on the shape of the spectrum. One can only observe these effects from highly resolvable spectra such as those shown in this paper.

Underlying the spectral features just discussed is a broad distribution of VSF intensity that extends over the full range observed here. This broad VSF intensity extending from 2800 cm^{-1} to 3800 cm^{-1} is attributed to the MSA proton continuum band and a low amplitude hydrogen bonding band. The broad bands of bulk and surface water from a neat water solution have also been attributed to a type of proton continuum since protons are quite mobile in liquid water. However, the tetrahedral structure and broad distribution of hydrogen bonding states giving rise to hydrogen bonding bands may be a more appropriate description for liquid water as discussed above in Section II. Since MSA is a strong acid, it continually undergoes dissociation and association of its acidic proton which gives rise to the proton transfer equilibria shown from 2800 cm^{-1} to 3800 cm^{-1}.[23] Similar continua have been observed in infrared and Raman spectra of condensed phase acids. Strong acids can be differentiated spectroscopically by their proton continuum, which is always broad yet unique to the acid. Proton continua have been also clearly observed in infrared spectra of liquid MSA and sulfuric acid.[38,41,42] This broad band for surface MSA (99+%, pK_a of -1.9,[42]) that begins before 2800 cm^{-1} (estimated peak fit at 2500 cm^{-1}) and extends and decreases uniformly beyond 3800 cm^{-1} indicates that proton transfer is occurring at the surface of MSA solutions.

To determine the orientation of the MSA molecule at the surface of the pure MSA solution, we have conducted VSFS polarization experiments. For the pure MSA solution, although we observed a broad SPS VSF intensity due to the surface water, there are no observed sharp resonances for the SPS (in-plane) CH_3-SS intensity as shown in the inset of Figure 3a. (Low signal to noise levels in the SPS spectra are evident in the lower energy region and are due to lower IR energies coupled with low SPS intensity.) From the SSP and the SPS spectra, the distribution of angles for the CH_3 of MSA is calculated to be 0 - 60 degrees from the surface normal (see Brown et al.[35] for VSF calculation methods). Additionally, the observed VSF SSP (out-of-plane) intensity of the CH_3-AS is small as is shown in Figure 3b. This is indicative of a CH_3 axis oriented parallel to the

surface normal suggesting a narrower angle distribution of the surface MSA. The symmetry axis of the methyl group is then on average pointing away from the solution surface into the gas phase and the SO_3^- moiety is solvated in the solution (MSA pK_a=-1.9,[42]).

The surface of aqueous solutions of differing MSA concentrations have been examined to provide further insight into the structure of surface MSA as well as the effect of MSA on the hydrogen bonding of surface water. The SSP VSF spectra in Figures 4a and 4b were taken of 0.02, 0.03, and 0.10 bulk mole fraction methane sulfonic acid (mf MSA) solutions, respectively. For ease of comparison with each other, the MSA spectra in Figure 4a are superimposed on the VSF spectra of neat water. We observe that the CH_3-SS peak at 2947 cm^{-1} increases in intensity with increasing MSA concentration. The area of the CH_3-SS peaks were fit to a Voigt function and the square root of this area intensity was compared relative to each solution. Shown in Figure 4c is the fit to the 0.1 mf MSA spectra which illustrates this procedure. The increase in number density calculated from the square root of VSF intensity is consistent with the increase in number density from the surface tension measurements. Recall that the square root of the VSF intensity is proportional to the orientationally averaged surface number density. Since the square root of the VSF tracks with the surface number density from the surface tension measurements, this indicates that the MSA surface orientation distribution from the VSF studies does not change significantly with changes in surface concentration. In addition, there are no frequency shifts observed with changing MSA surface concentration for the CH_3-SS peak. Such frequency shifts of methyl moieties were observed for similar VSF studies of dimethyl sulfoxide and were attributed to increased crowding at the interface and a subsequent change in molecular orientation. The lack of observed VSFS frequency shifts for the well resolved CH_3-SS peak of MSA and its interference edge strongly supports that although the surface environment and surface concentration are changing, the average orientation of the surface MSA is not. The lack of spectral shift suggests that interactions between adjacent MSA surface molecules does not significantly perturb the molecular structure of surface MSA.

In Figures 4a and 4b, additional significant spectral features are observed that provide information about the structure of water at the surface of these MSA solutions. The destructive interference between the VSF response of the CH_3-SS and the CH_3-AS that was previously discussed, is clearly evident in the VSF spectra and remains relatively unchanged with changing MSA concentration. First, in the region from 2900 cm^{-1} to 3050 cm^{-1}, an increase in the broad hydrogen bonding band intensity with increasing MSA concentration is observed. This is consistent with an increase in protonated water species present as the solution concentration becomes more highly acidic. Secondly, the entire hydrogen bonding and dangling OH region from 3000 to 3800 cm^{-1} is significantly affected with small increases in the MSA concentration. The hydrogen bonding broad band of the 0.02 mf MSA spectra (Figure 4a) maintains its intensity in the 3190 cm^{-1} region relative to the spectrum of neat water, while the 3400 cm^{-1} region decreases in intensity. In the 0.03 mf MSA (Figures 4a-b), the 3400 cm^{-1} region continues to decrease in intensity more than the 3190 cm^{-1} region. The surface-water broad band is dominated by the 3190 cm^{-1} region at the expense of the 3400 cm^{-1} region with increasing MSA concentration.

Recall from the surface tension measurements discussed in section I that MSA molecules partition to the surface of aqueous solutions, effectively displacing a large number of the surface water molecules. In the VSF spectra (Figures 4a –b) the lower intensity of the hydrogen bonding region and the eventual loss of the free OH peak reflects the lower number density of the surface water. The observed large intensity shift to lower energies in the spectra relative to the neat water surface indicates that there is an increase in the intermolecular in-phase hydrogen bonding interactions of the remaining surface water molecules, i.e. there is a loss of the more weakly hydrogen bonded water species in addition to the loss of surface water via MSA displacement. Thus the number of water molecules with weaker hydrogen bonding character disappear and as the MSA concentration is increased, the remaining surface water molecules are more highly correlated resulting in stronger in-phase intermolecular hydrogen bonding vibrational character. An increased in-phase correlation and resultant net alignment caused by the surface MSA is consistent with the fact that MSA is highly acidic. Since the MSA anions

are surface active as established by both the surface tension and VSFS data, a net negative charge exists at the uppermost portion of the solution surface. The anion's counterpart, the H_3O^+ (or $H_5O_2^+$) cation, is stabilized in the surface region by the ionic interaction with the surface methane sulfonate anions. Thus, there is a resultant electrostatic field formed by these two species at the surface of aqueous MSA solutions producing a tight double layer. Previous VSF studies of negatively charged surfactants have shown significantly large increases in the VSF signal strength of the in-phase hydrogen bonding spectral region.[43] This enhancement was primarily due to the formation of a double layer, effectively extending the interfacial region. Due to the concentrations and ionic strengths in our MSA studies, the relatively thin double layer that is formed does not significantly increase the interfacial depth. Thus, there is no appreciable VSF intensity increase observed in the surface water region of the MSA solutions.

In the dangling OH bond region shown in Figure 4a, the $OH_{(da)}$ stretch decreases in intensity with increasing MSA concentration. Given that the square root of the VSF intensity is proportional to the number of orientationally-averaged molecules at the surface, we have compared the square root of the free OH peak areas and find that the number of free OH species has been reduced by ~75% for the 0.02 MSA mf solution surface relative to the free OH density at the surface of neat water. Another addition of MSA to solution, the 0.03 MSA mf solution, results in a ~90% depletion of surface free OH species. In the 0.10 mf MSA solution (Figure 4b) the $OH_{(da)}$ peak is below detection limits. These results suggest that close to three-fourths, and nine-tenths of the neat water surface $OH_{(da)}$ bonds in the 0.02 and 0.03 mf MSA solutions, respectively, are now fully coordinated to the remaining surface water molecules, and that by 0.10 MSA mf (0.5 mf_e), there is no evidence of free OH species. These results indicate that although 50 % - 85 % of the surface is composed of water for the solution concentrations studies here, the surface structure is controlled by the surface MSA molecules.

The VSF spectrum of 0.10 mf MSA in the hydrogen bonding region of water appears to be different than the lower concentration spectra of 0.02 and 0.03 mf MSA in the water

spectral region. In Figure 4b, the 0.10 mf MSA VSF spectrum is plotted with the 0.03 mf MSA spectrum for ease of comparison. The predominant difference observed in the 0.10 mf spectra is the decrease in the VSF intensity in the broad hydrogen bonding region, consistent with the surface tension data that shows at 0.10 mf the surface ratio of MSA : H_2O is 1. The lower VSF intensities suggest that there are fewer water molecules at the surface consistent with the effective surface mole fraction (mf_e) discussed in section I. There are 3 important points to note regarding this spectrum. Although the water region is less intense, the shape is still indicative of a more highly correlated surface water region. This is a result from the MSA persisting in the form of methane sulfonate surface ions, thereby creating an electrostatic field as previously discussed. Secondly, the VSF intensity of the CH_3-SS at 2947 cm^{-1} is increased as is expected from the increasing MSA surface concentration from the 0.10 mf solution. Thirdly, the square-shaped intensity drop that was first observed from Figure 3 (neat MSA) from destructive interference between the CH_3-SS and the CH_3-AS is significantly distorted. The effect is clearest in the 0.10 mf spectrum of Figure 4b, although it is also evident in the 0.02 and the 0.03 mf MSA solution spectra shown in Figures 4a-b. Accompanying this intensity drop is the asymmetric shape of the CH_3-SS, with a much sharper drop on the high energy side of the spectrum. Within the square shaped intensity drop, we observe a small peak at ~2980 cm^{-1}. There is evidence in gas and condensed phase studies that MSA dimer species (CH_3SO_3-H-O_3SCH_3) would give rise to a resonance at 2977 cm^{-1}.[38] In the peak fit shown in Figure 4c, a small 2980 cm^{-1} peak has been included in the fit, but we have also been able to reproduce a similar small peak from changing the surrounding peak parameters in this region without including the 2980 cm^{-1} peak. Thus, with the fitting calculations taking into account the VSF phase information, we cannot say with certainty that the surface MSA dimer exists at the surface of the 0.1 mf MSA solution. If the surface MSA dimer species does exist, the small peak intensity suggests that its surface concentration may be low.

IV. Binary versus Ternary solutions: Sulfuric acid, MSA, and Water

Ternary mixtures of sulfuric acid (SA), MSA, and water were studied to help shed light on the surface structures of more complex systems that also have relevance to atmospheric aerosol chemistry. VSF spectra of a 0.03 and a 0.05 mf MSA in a 75 weight % sulfuric acid (SA) solution (1 SA : 2 H_2O molecules) are shown in Figure 5a. (0.03 and 0.05 mf MSA bulk concentrations correspond to approximate bulk ratios of 1 MSA : 11 SA : 22 H_2O and 1 MSA: 6 SA : 13 H_2O molecules, respectively.) The sulfuric acid proton continuum shown in Figure 5a dominates the VSF spectra of the 0.03 and 0.05 mf MSA/SA solutions from 2800 to ~3400 cm^{-1} and this continuum is comparable in shape and intensity to the surface spectrum of the 96 % SA solution shown in the inset of Figure 5a. The CH_3-SS peak from MSA is observed at 2947 cm^{-1}, riding on top of the continuum intensity. There are no frequency shifts for the CH_3-SS observed for this mode relative to the pure and binary MSA mixture VSF studies. The sharp decrease in intensity is still observable on the high frequency side of the CH_3-SS, indicating the destructive interference is still occurring as one would expect. From the VSF spectra of the 0.03 mf and the 0.05 mf MSA/SA solutions, an approximate doubling of the CH_3-SS VSF intensity is observed, indicating that MSA is partitioning to the surface. This is similar to the partitioning from a purely aqueous solution. (Lack of SPS intensity in experiments probing the CH_3-SS region indicated that reorientation of the CH_3 is neglibible and therefore the square root of the VSF intensity can be directly correlated to surface number density.) In the proton continuum region, we do not observe any distinct features other than the dominant proton transfer equilibria, i.e. resonances from the protonated water species, $H_5O_2^+$ and/or H_3O^+. The shift in energy of the proton continuum from the MSA (Figure 3) to SA (Figure 5a inset) is consistent with the more highly acidic SA species relative to MSA.[44,41] What is important to note is that similar interference features are seen in the binary and the ternary solution spectra.

The spectra of MSA in aqueous versus sulfuric acid solutions are compared and shown in Figure 5b in order to understand the differences in surface structure of both MSA and water at these two different surfaces. It is observed from the spectra in Figure 5b that the VSF intensity from the CH_3-SS peak of MSA is reduced for the ternary mixture, and we

do not observe a frequency shift for the CH_3-SS for the two solutions. The lower CH_3-SS SSP VSF intensity of the ternary mixture in this region indicates that the MSA surface molecules are being displaced by sulfuric acid and/or sulfuric acid complexes. Reorientation for the CH_3 of MSA in the 0.1 mf MSA/SA solution can be eliminated based on the lack of SPS VSF intensity in our studies of the CH_3-SS spectral region. The lack of frequency shift for this mode indicates that the local structure of the remaining surface CH_3 groups of MSA is not changing significantly. Clearly, sulfuric acid is much more efficient at displacing the methane sulfonic acid from the surface compared to water, and therefore the MSA molecules partition less effectively to the surface in a 75 weight % sulfuric acid aqueous solution.

Conclusions

Methane sulfonic acid adsorption and molecular structure at the surface of aqueous solutions including 75 weight percent sulfuric acid have been studied using vibrational sum frequency spectroscopy. Methane sulfonic acid (pK_a -1.9) is a strong acid and below 0.2 mf MSA in aqueous solution, MSA is dissociated from its acidic hydrogen in bulk solution. Surface tension and VSF polarization experimental results indicate that MSA is preferentially adsorbed at the surface of aqueous solutions. The methyl group of MSA is oriented away from the liquid state and this orientation does not change significantly with changing surface concentration. We calculate the angle of the C-S bond which bisects the MSA molecule to be in a distribution from 0-60 degrees from the surface normal. Surface water structure was also studied using VSFS. With small amounts of MSA added to bulk-water, the surface-water structure becomes even more symmetrically coordinated with stronger intermolecular correlation of hydrogen bonds. Surface free OH species are significantly depleted from the surface of MSA solutions even at low concentrations. In ternary mixtures of MSA, sulfuric acid, and water, sulfuric acid displaces the surface MSA more efficiently than water does from the surface of a binary solution of MSA and water. Thus, heterogeneous chemistry of MSA solutions, which has application to the heterogeneous chemistry of atmospheric aerosols, may be distinctly different from what is observed for the bulk liquid-phase chemistry. This conclusion is based on the fact that heterogeneous chemistry begins with surface adsorption. A highly oriented methyl

barrier at the surface of a solution, and an altered surface water structure depleted in surface free OH bonds, will influence gas phase adsorption character and thereby may alter reaction pathways.

References

(1) Davis, D.; Chen, G.; Kasibhatla, P.; Jefferson, A.; Tanner, D.; Eisele, F.; Lenschow, D.; Neff, W.; Berresheim, H. *J. Geophys. Res.* **1998**, *103*, 1657-1678.

(2) Schwartz, S. E.; Andreae, M. O. *Science* **1996**, *272*, 1121-0.

(3) Charlson, R. J.; Lovelock, J. E.; Andreae, M. O.; Warren, S. G. *Nature* **1987**, *326*, 655-661.

(4) Charlson, R. J.; Schwartz, S. E.; Hales, J. M.; Cess, R. D.; Coakley, J., J. A.; Hansen, J. E.; Hofmann, D. J. *Science* **1992**, *255*, 423-430.

(5) De Bruyn, W. J.; Shorter, J. A.; Davidovits, P.; Worsnop, D. R.; Zahniser, M. S.; Kolb, C. E. *J. Geophys. Res.* **1994**, *99*, 16,927-16,932.

(6) Richter, L. J.; Petralli-Mallow, T. P.; Stephenson, J. C. *Optics letters* **1998**, *23*, 1594-1596.

(7) Vogel, A.; Noack, J.; Nahen, K.; Theisen, D.; Busch, S.; Parlitz, U.; Hammer, D. X.; Noojin, G. D.; Rockwell, B. A.; Birngruber, R. *Applied Physics B, Lasers and Optics* **1999**, *68*, 271-280.

(8) Gragson, D. E.; McCarty, B. M.; Richmond, G. L. *J. Opt. Soc. Am. B* **1996**, *13*, 2075-2083.

(9) Gragson, D. E.; Alavi, D. S.; Richmond, G. L. *Optics Letters* **1995**, *20*, 1991-1993.

(10) Allen, H. C.; Gragson, D. E.; Richmond, G. L. *J. Phys. Chem. B* **1999**, *103*, 660-666.

(11) Kipling, J. J. Ch. 11. Adsorption at the Liquid-Vapour Interface. In *Adsorption from Solutions of Non-Electrolytes*; Kipling, J. J., Ed.; Academic Press, Inc.: New York, 1965; pp 191-217.

(12) Allen, H. C.; Raymond, E. A.; Brown, M. G.; Richmond, G. L. *submitted* **2000**.

(13) Miranda, P. B.; Shen, Y. R. *J. Phys. Chem. B* **1999**, *103*, 3292-3307.

(14) Raduge, C.; Pflumio, V.; Shen, Y. R. *Chemical Physics Letters* **1997**, *274*, 140-144.

(15) Du, Q.; Superfine, R.; Freysz, E.; Shen, Y. R. *Phys. Rev. Lett.* **1993**, *70*, 2313-2316.

(16) Schnitzer, C.; Baldelli, S.; Shultz, M. J. *J. Phys. Chem. B* **2000**, *104*, 585-590.

(17) Schnitzer, C.; Baldelli, S.; Campbell, D. J.; Shultz, M. J. *J. Phys. Chem. A* **1999**, *103*, 6383-6386.

(18) Schnitzer, C.; Baldelli, S.; Shultz, M. J. *Chem. Phys. Lett.* **1999**, *313*, 416-420.

(19) Simonelli, D.; Baldelli, S.; Shultz, M. J. *Chem. Phys. Lett.* **1998**, *298*, 400-404.

(20) Baldelli, S.; Schnitzer, C.; Shultz, M. J. *Chem. Phys. Lett.* **1999**, *302*, 157-163.

(21) Baldelli, S.; Schnitzer, C.; Shultz, M. J.; Campbell, D. J. *Chem. Phys. Lett.* **1998**, *287*, 143-147.

(22) Baldelli, S.; Schnitzer, C.; Shultz, M. J.; Campbell, D. J. *J. Phys. Chem. B* **1997**, *101*, 10435-10441.

(23) Zundel, G. Chapter 15. In *The Hydrogen Bond II. Structure and Spectroscopy*; Schuster, P., Zundel, G., Sandorfy, C., Eds.; North-Holland Publishing Company: New York, 1976; Vol. 2; pp 687-766.

(24) Falk, M.; Giguere, P. A. *Can. J. Chem.* **1957**, *35*, 1195-1204.

(25) Goss, L. M.; Sharpe, S. W.; Blake, T. A.; Vaida, V.; Brault, J. W. *J. Phys. Chem. A* **1999**, *103*, 8620-8624.

(26) Buch, V.; Devlin, J. P. *J. Chem. Phys.* **1999**, *110*, 3437-3443.

(27) Walrafen, G. E.; Yang, W.-H.; Chu, Y. C. Ch. 21 Raman evidence for the clathratelike structure of highly supercooled water. In *Supercooled Liquids*; American Chemical Society:, 1997; pp 287-308.

(28) Devlin, J. P.; Buch, V. *J. Phys. Chem.* **1995**, *99*, 16534-16548.

(29) Hare, D. E.; Sorenson, C. M. *J. Chem. Phys.* **1990**, *93*, 25-33.

(30) Whalley, E.; Klug, D. D. *J. Chem. Phys.* **1986**, *84*, 78-80.

(31) Scherer, J. R. Chapter 3. The vibrational spectroscopy of water. In *Advances in Infrared and Raman Spectroscopy*; Clark, R. J. H., Hester, R. E., Eds.; Heyden: Philadelphia, 1978; Vol. 5; pp 149-216.

(32) Giguere, P. A. *J. Chem. Phys.* **1987**, *87*, 4835-4840.

(33) Walrafen, G. E.; Chu, Y. C. *J. Phys. Chem.* **1995**, *99*, 11225-11229.

(34) Buch, V.; Devlin, J. P. *J. Chem. Phys.* **1991**, *94*, 4091-4092.

(35) Brown, M. G.; Raymond, E. A.; Richmond, G. L. **2000**.

(36) Wolfrum, K.; Laubereau, A. *Chem. Phys. Lett.* **1994**, *228*, 83-88.

(37) Crowell, R. A.; Holtom, G. R.; Xie, X. S. *J. Phys. Chem.* **1995**, *99*, 1840-1842.

(38) Chackalackal, S. M.; Stafford, F. E. *Journal of the American Chemical Society* **1966**, *88*, 4815-4818.

(39) Hirose, C.; Akamatsu, N.; Domen, K. *Applied Spectroscopy* **1992**, *46*, 1051-1072.

(40) Hirose, C.; Akamatsu, N.; Domen, K. *J. Chem. Phys.* **1992**, *96*, 997-1004.

(41) Tomikawa, K.; Kanno, H. *J. Phys. Chem. A* **1998**, *102*, 6082-6088.

(42) Langner, R.; Zundel, G. *J. Chem. Soc., Far. Trans.* **1998**, *94*, 1805-1811.

(43) Gragson, D. E.; McCarty, B. M.; Richmond, G. L. *J. Am. Chem. Soc.* **1997**, *119*, 6144-6152.

(44) Habeeb, M. M. *Applied Spectroscopy Reviews* **1997**, *32*, 103-140.

Figure Captions

Figure 1a. Surface tension measurements of aqueous MSA solutions. b. Bulk number density, Gibbs surface excess, and surface number density of aqueous MSA solutions. The surface of MSA aqueous solutions, particularly at low concentrations, is enriched in MSA relative to the bulk MSA concentration.

Figure 2. SSP VSF spectrum of the surface of neat water. The broad hydrogen bonding band extends below 2900 cm^{-1} to ~ 3550 cm^{-1}. The dangling OH (free OH) and the gas phase AS are observed at 3702 cm^{-1} and 3760 cm^{-1}, respectively.

Figure 3a. SSP VSF spectrum of the surface of neat MSA which includes the CH_3-SS at 2947 cm^{-1} and the broad MSA proton continuum. Inset: SPS (in-plane) VSF spectrum of the surface of neat MSA. b. Fit to the data taking into account the relative VSF phase. The destructive interference (opposing phases) between the CH_3-SS and the CH_3-AS is clearly observed between 2950 and 3025 cm^{-1}.

Figure 4a. SSP VSF spectra of the surface of 0.02 and 0.03 mf MSA in water. The neat surface water spectrum is shown for comparison. Note the depletion of the free OH with increasing MSA concentration and that the hydrogen bonding region (3000- 3500 cm^{-1}) is significantly changing in shape and frequency distribution with increasing MSA concentration. b. SSP VSF spectrum of the surface of 0.10 mf MSA. The 0.03 mf MSA is shown for ease of comparison. c. Fit to the 0.1 mf MSA SSP VSF spectrum.

Figure 5a. SSP VSF spectra of 0.05 mf MSA and 0.03 mf MSA in 75 weight percent sulfuric acid aqueous solution. Inset: SSP VSF spectrum of 96-weight % sulfuric acid. b. VSF SSP spectrum of 0.10 mf MSA in 75 weight percent sulfuric acid aqueous solution. SSP VSF spectrum of 0.10 mf MSA in water is shown here for ease of comparison.

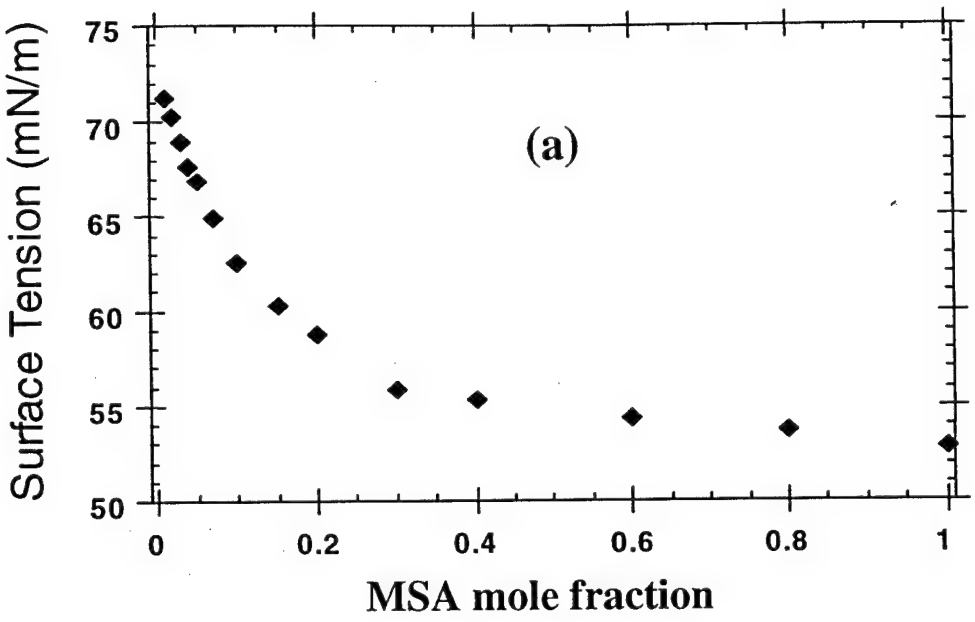
Surface Tension (mN/m)
75
70
65
60
55
50
(a)
0
0.2
0.4
0.6
0.8
1
MSA mole fraction

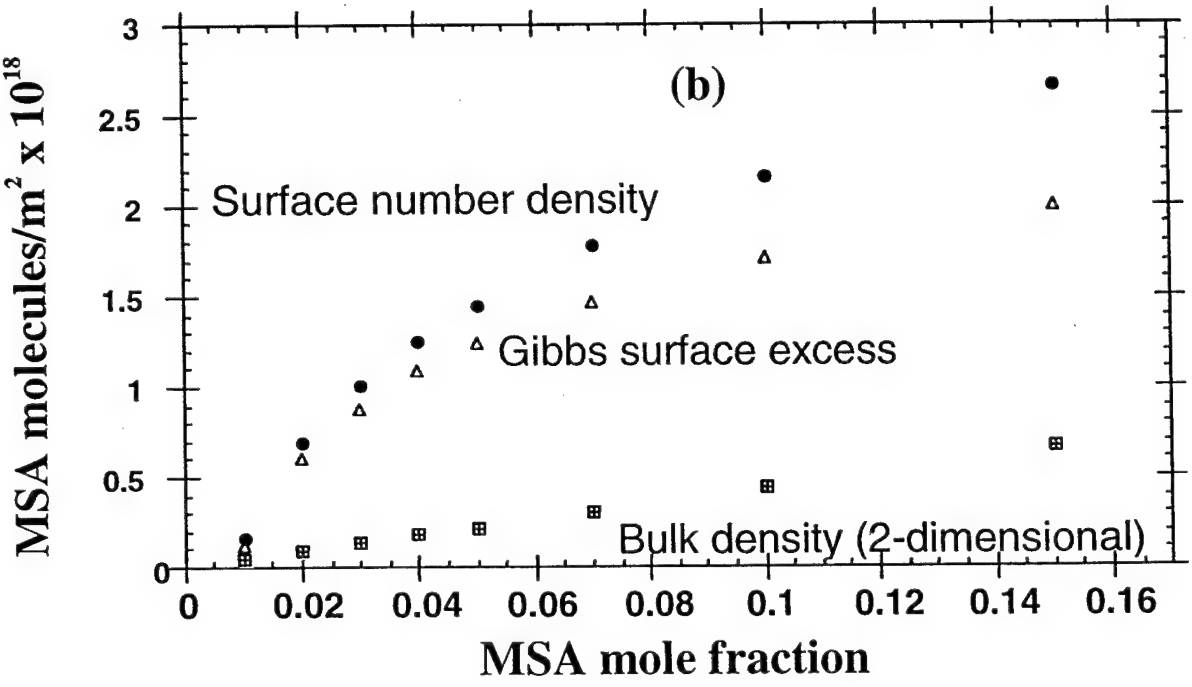
MSA molecules/m^2 x 10^{18}
3
2.5
2
1.5
1
0.5
0
(b)
Surface number density
Gibbs surface excess
Bulk density (2-dimensional)
0
0.02
0.04
0.06
0.08
0.1
0.12
0.14
0.16
MSA mole fraction

Fig 1

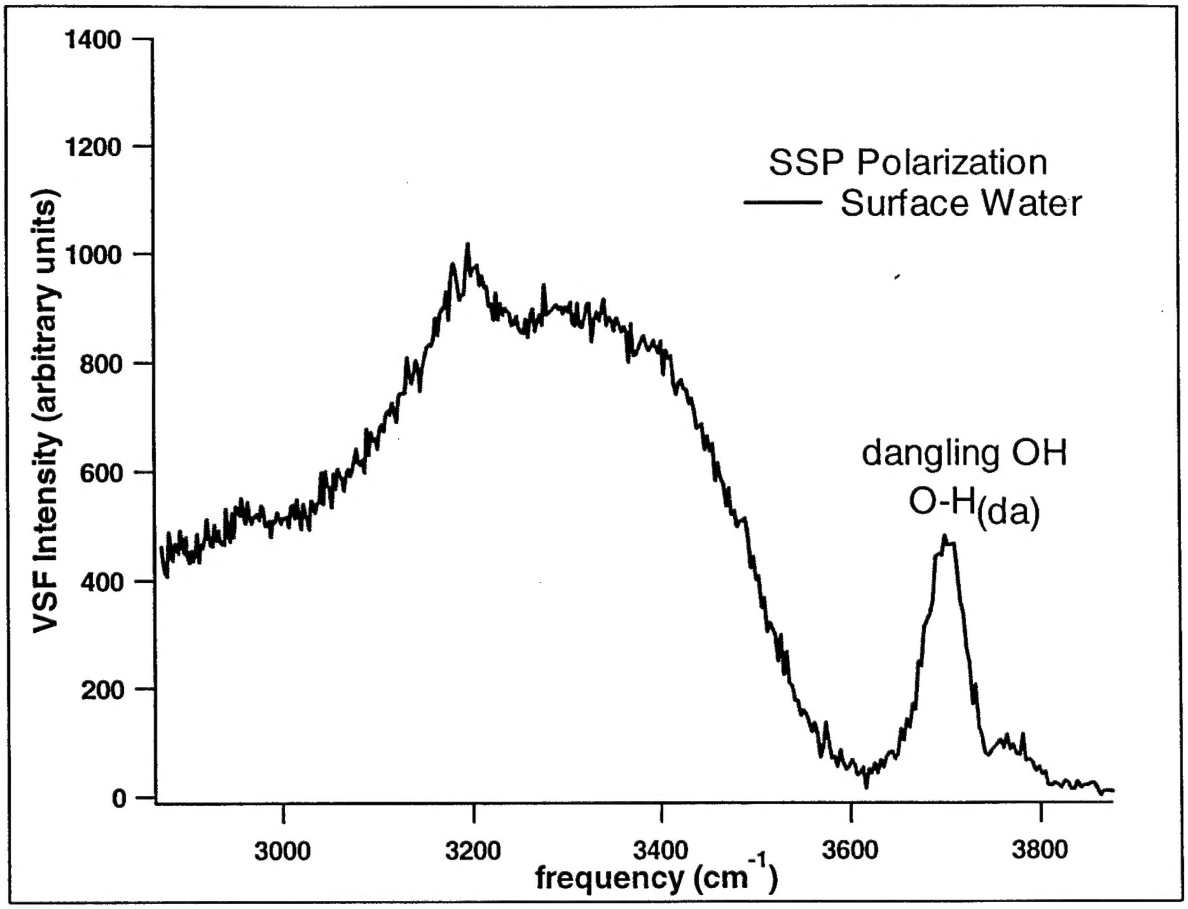
1400
1200
1000
800
600
400
200
0
VSF Intensity (arbitrary units)
SSP Polarization
Surface Water
dangling OH
O-H(da)
3000
3200
3400
3600
3800
frequency (cm-1)

Fig 2

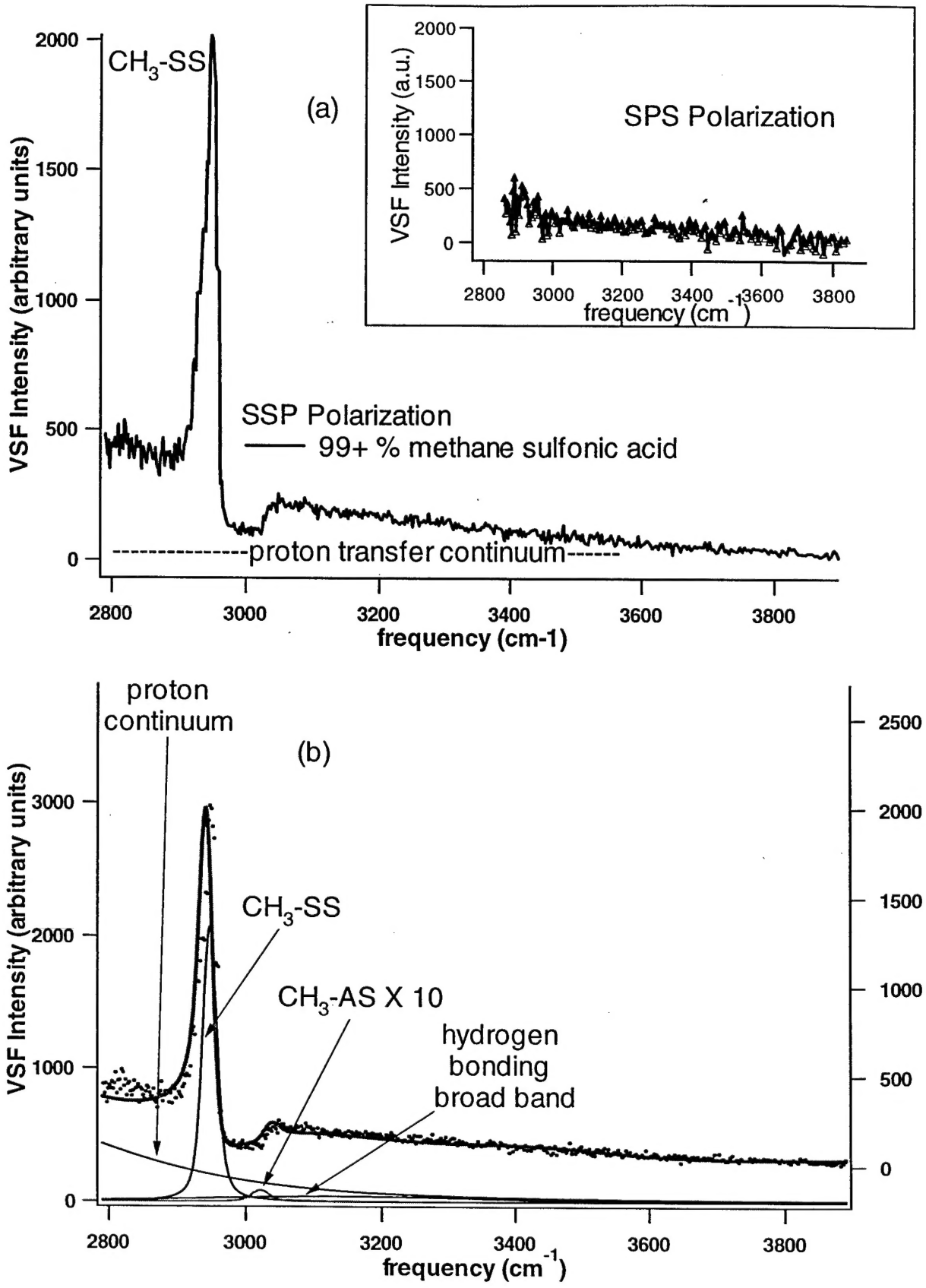
CH3-SS
(a)
SPS Polarization
VSF Intensity (a.u.)
frequency (cm-1)
SSP Polarization
99+ % methane sulfonic acid
proton transfer continuum
VSF Intensity (arbitrary units)
frequency (cm-1)
proton continuum
(b)
CH3-SS
CH3-AS X 10
hydrogen bonding broad band
VSF Intensity (arbitrary units)
frequency (cm-1)

Fig 3

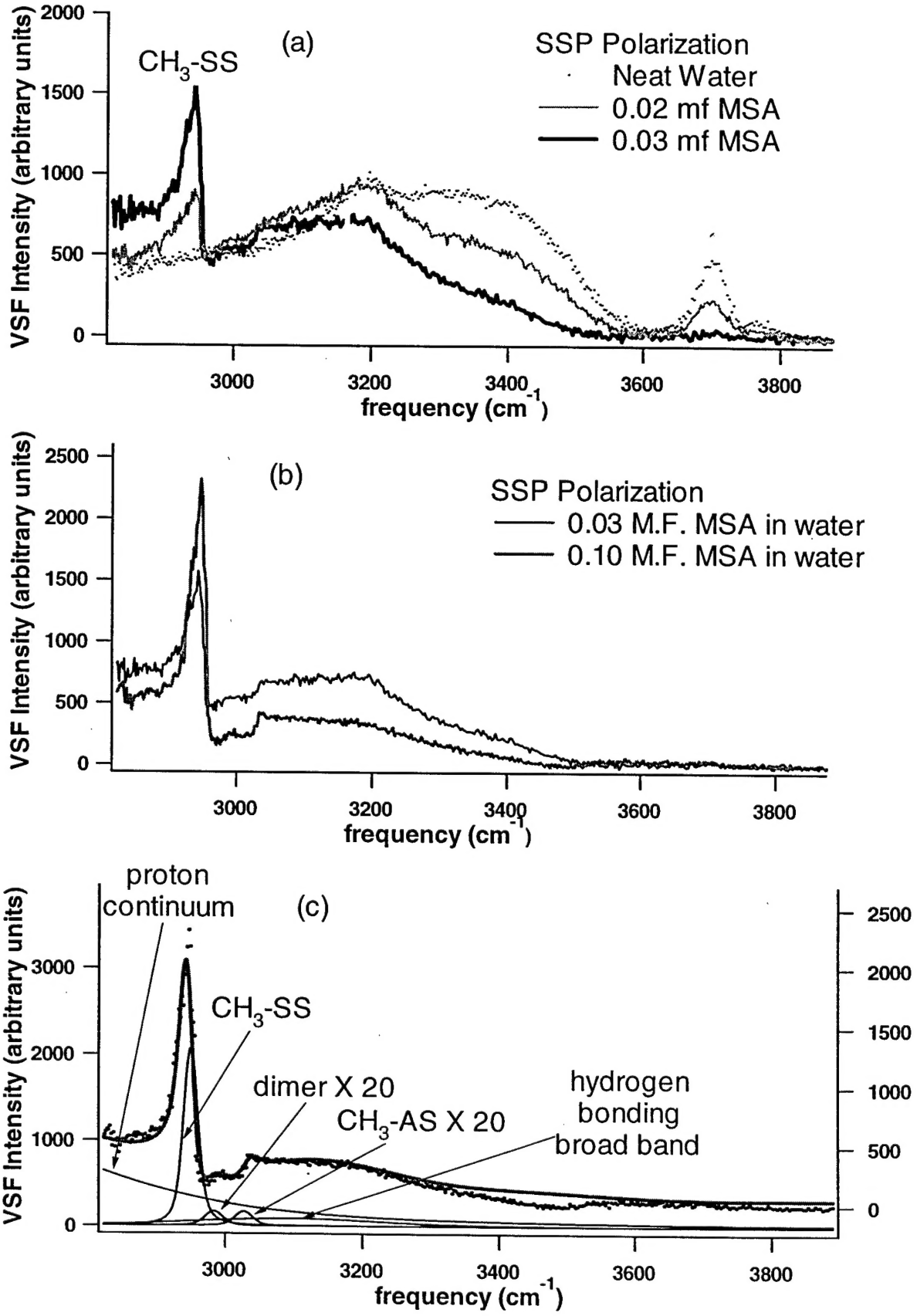
(a)
CH3-SS
SSP Polarization
Neat Water
0.02 mf MSA
0.03 mf MSA
VSF Intensity (arbitrary units)
frequency (cm-1)
(b)
SSP Polarization
0.03 M.F. MSA in water
0.10 M.F. MSA in water
VSF Intensity (arbitrary units)
frequency (cm-1)
proton continuum
(c)
CH3-SS
dimer X 20
CH3-AS X 20
hydrogen bonding broad band
VSF Intensity (arbitrary units)
frequency (cm-1)

Fig 4

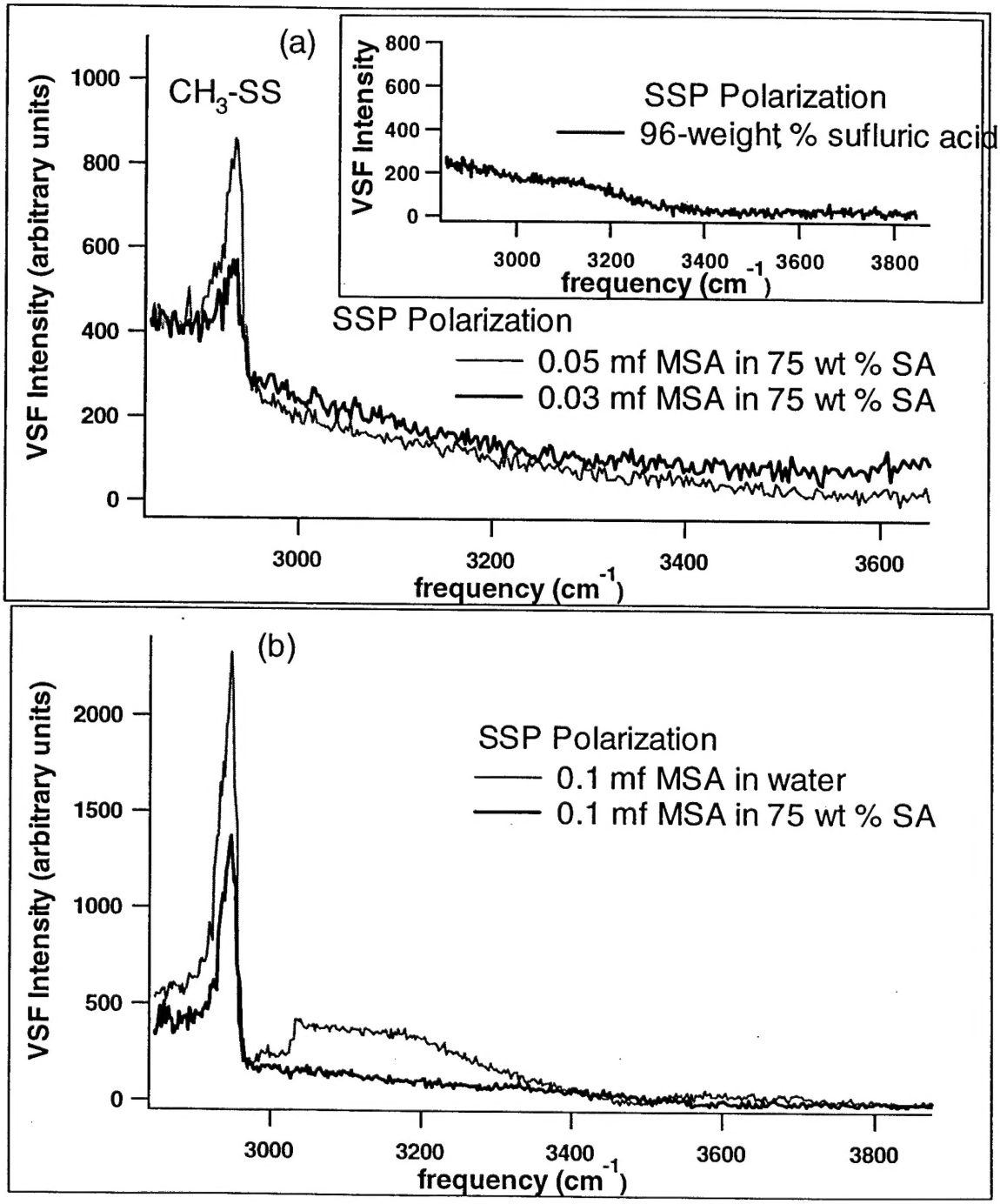
(a)
CH_3-SS
VSF Intensity (arbitrary units)
1000
800
600
400
200
0
3000
3200
3400
3600
frequency (cm^{-1})
SSP Polarization
0.05 mf MSA in 75 wt % SA
0.03 mf MSA in 75 wt % SA
VSF Intensity
800
600
400
200
0
3000
3200
3400
3600
3800
frequency (cm^{-1})
SSP Polarization
96-weight % sufluric acid
(b)
VSF Intensity (arbitrary units)
2000
1500
1000
500
0
3000
3200
3400
3600
3800
frequency (cm^{-1})
SSP Polarization
0.1 mf MSA in water
0.1 mf MSA in 75 wt % SA

Fig 5